

Study of the Imaging Properties of Retro-reflective Materials Used in Head-Mounted Projective Displays (HMPDs)

Hong Hua¹, Chunyu Gao¹, and Jannick P. Rolland²

¹Beckman Institute, University of Illinois at Urbana-Champaign, Urbana, IL 61801

²School of Optics/CREOL, University of Central Florida, Orlando, FL 32816

E-mail: honghua@uiuc.edu

ABSTRACT

The concept of head-mounted projective display (HMPD) has been recently proposed as an alternative to conventional eyepiece-type head-mounted displays (HMDs). An HMPD consists of a pair of miniature projection lenses and flat panel displays mounted on the head and retro-reflective sheeting material placed strategically in the environment. Recent efforts have been made to demonstrate the feasibility of the imaging concept and prototypes have been built. Our research indicates that the quality and properties of the retro-reflective material play critical roles in the overall imaging quality of HMPDs. The retro-reflective sheeting material is commonly used in traffic control and photonic lighting systems, rather than optimized for imaging purpose as in the HMPDs. The size and shape of the microstructures cause artifacts on images. In this paper, we will mainly focus on the evaluation of the various existing retro-reflective materials, and the examination of the impact of the material characteristics on imaging properties. The basic structures of the existing materials are briefly reviewed, the characteristic parameters used to quantify the material properties are defined, and a few samples are evaluated. The characteristics of interest include: the size and shape of the microstructure, the distribution pattern and density of the microstructure, retro-reflectivity, the profile of the reflected light, diffraction artifacts and ghost imaging. Finally, a comprehensive analysis are presented to examine how the material characteristics play their roles in an imaging system, such as the HMPD, and predict the imaging artifacts caused by these characteristics.

KEYWORDS: Head-mounted Projective Displays (HMPD), Head-mounted displays (HMD), Retro-reflection, Retro-reflective material, Augmented reality (AR).

1. INTRODUCTION

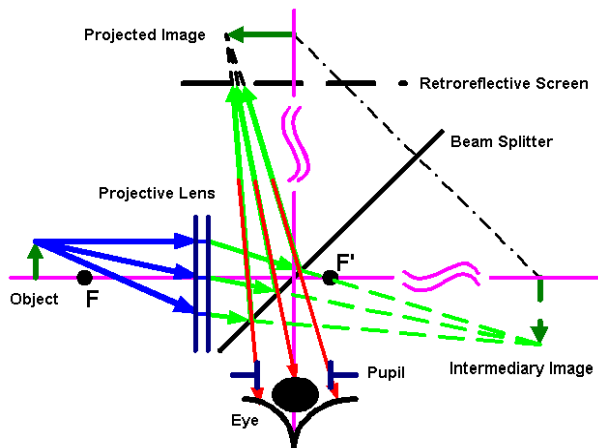


Fig.1 Imaging concept of HMPD

A head-mounted projective display (HMPD), conceptually illustrated in Fig.1, consists of a pair of miniature projection lenses, beam splitters, miniature displays mounted on the head, and a supple and non-distorting retro-reflective sheeting material placed strategically in the environment.^{1,2} An image on the miniature display, which is located beyond the focal point of the lens rather than between the lens and the focal point as in a conventional head-mounted display (HMD), is projected through the lens and retro-reflected back to the entrance pupil of the eye, where the exit pupil of the projection optics is conjugated to through the beam splitter, so the eye can observe the projected image.

Two major components, the projective optics rather than an eyepiece as used in conventional HMDs and a retro-reflective screen rather than a diffusing screen as used in other projection-based displays,³ distinguish the HMPD technology from conventional HMDs and stereoscopic projection displays such as CAVEs.^{4, 5} The usage of projection optics allows for a larger field of view (FOV) and less optical distortion, compared with conventional eyepiece-based optical see-through HMDs.⁶ Furthermore, the combination of projection and retro-reflection makes the HMPD intrinsically provides correct occlusion of computer-generated virtual objects by real objects. Ideally, the perception of image shape and location is independent of the shape and location of a retro-reflective screen. Thus, the technology has been pursued as an alternative to stereoscopic displays for a variety of 3D visualization applications.⁷⁻⁹

The quality and properties of the retro-reflective material play critical roles in the overall imaging quality of HMPDs. The retro-reflective sheeting material is commonly used in traffic control and photonic lighting systems, rather than optimized for imaging purpose as in the HMPDs. The size and shape of the microstructures cause artifacts on image. The subject of this paper is to evaluate the various existing retro-reflective materials and examine the impact of the material characteristics on imaging artifacts. We will briefly review the related research in section 2, review the basic structures of the existing materials in section 3, evaluate a few representative samples in section 4, and examine how material characteristics play their roles in an imaging system, such as the HMPD and predict the imaging artifacts in section 5.

2. RELATED WORK



Fig. 2 HMPD prototype

The HMPD concept was initially presented by Kijima and Ojika, while a patent was also issued on the conceptual idea of the display to Fergason.^{1, 2} Kawakami et al. and Inami et al. developed a configuration named X'tal Vision and proposed the concepts of object-oriented displays and visual-haptic displays.^{7, 10} Independently, the HMPD technology was developed as a tool for medical visualization by Parsons and Rolland.¹¹ Hua et al. have made efforts to demonstrate the feasibility of the HMPD imaging concept and to quantify some of the properties and behaviors of the retro-reflective materials in imaging systems.^{3, 8} The authors have furthered the efforts with an ultra-light, high quality projection lens by introducing a diffractive optical element (DOE) as well as plastic components, implemented a compact prototype using the custom-designed lens, and investigated the applications of the HMPD technology in distance collaborative augmented environments.^{8, 12} The

prototype achieves 52 degrees FOV and weighs about 750 grams. Figure 2 shows the front view of the prototype.

3. RETRO-REFLECTIVE MATERIAL

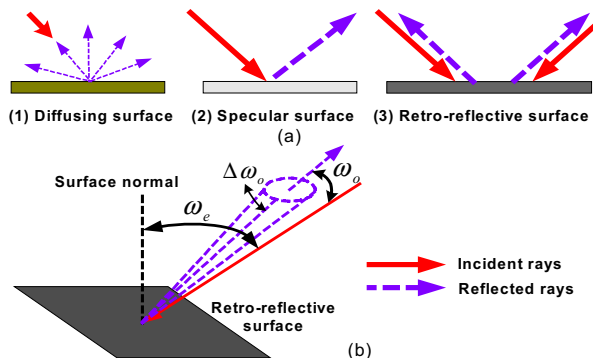


Fig. 3 Retro-reflection and retro-reflective material: (a) Difference in retro-reflection from diffusing and specular reflections; (b) Performance of retro-reflective material

The difference between retro-reflective surfaces and diffusing or specular surfaces lies in the fact that rays hitting a retro-reflective surface at any angle are reflected back on themselves in the opposite direction (Fig. 3-a). In HMPDs, this indicates that the perception of image shape and location is independent of the shape and location of a retro-reflective screen (i.e. the screen placement is transparent to the user).

Two kinds of retro-reflective materials are well known: corner cube arrays and micro-bead arrays

(Fig. 4). Micro-bead arrays utilize specular reflection while corner cube arrays utilize total internal reflection (TIR). Thus corner cube is expected to have higher reflectivity than micro-bead. We have gathered more than

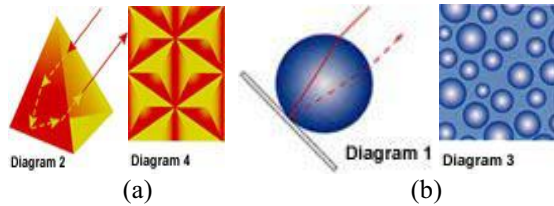


Fig. 4 Retro-reflective materials: (a) micro-corner cube array; (b) micro-bead array.

10 different samples. Figures 5-a through 5-d show the microstructures of four representative samples (4-mm-thick round plate, 4-mm-thick triangular plate, flexible thin film, and fabric, respectively). The samples 5-a and 5-b are corner-cube rigid plates which mold cube-arrays on a 2-mm plastic substrate, the sample 5-c is corner-cube film which shapes cube-arrays on a plastic film, and the sample 5-d is micro-bead fabric which paints glass-beads on the surface of fabric.

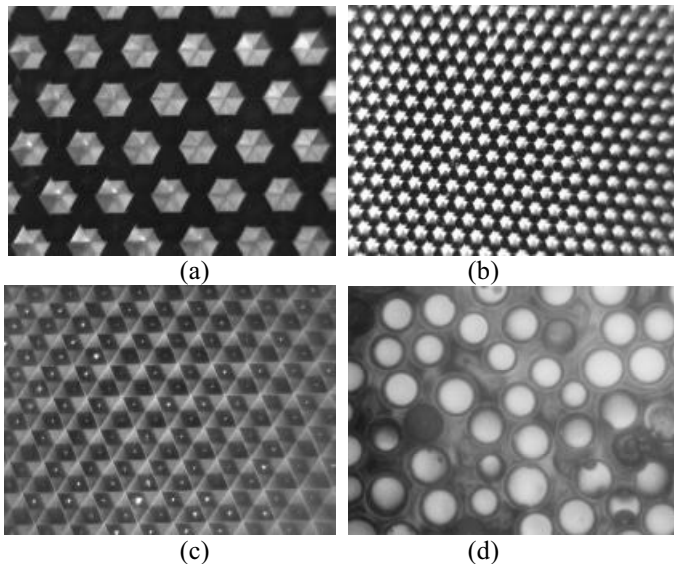


Fig. 5 Micro-structures of representative samples

Among the samples, sample 5-b and 5-c, subjectively, are the best in terms of image brightness and imaging quality. The sample 5-b is a rigid plate in the shape of 280 mm equilateral triangle. This sample is expensive to make a large size screen, but is very good for making flat screens, such as a tabletop screen. The sample 5-c is a kind of flexible 1-meter wide film with adhesion at the back, which is inexpensive, easy to clean, and very good for irregularly shaped screens.

The retro-reflective materials are typically not optimized for imaging optics. Based on observations, we inferred that the size and shape of the microstructures cause artifacts on imaging quality. A series of experiments have been designed to quantify the sample materials in

terms of: the physical structures (e.g. size, shape, distribution pattern, and density of the microstructure); reflective properties (e.g. the profile of the reflected light, and retro-reflectivity measurement); and other optical properties related to image quality (e.g. diffraction artifacts, and specular reflections). Details about the experiments and observations are discussed in the next section.

4. EVALUATING RETRO-REFLECTIVE SAMPLE MATERIALS

4.1. Physical structures

Examining the microscopic images 5-a through 5-c, we observed that the physical structures of these samples have significant difference in size, density, and pattern. The cube size of the samples 5-a through 5-c is 0.864mm, 0.254mm, and 0.165mm, respectively. The average bead size of the sample 5-d is 0.1mm. In the microscopic images, we inferred that the retroreflective portion of a corner-cube is corresponding to the dark regions, while the non-retroreflective portion of a cube is corresponding to the bright regions. This observation is not applicable to the micro-bead sample since it is based on a different principle. We observed that two adjacent cubes in the sample 5-a and 5-b barely have gaps, while sample 5-c has noticeable gaps (approximately 5 to 10 microns), thus samples 5-a and 5-b have denser structure than the sample 5-c. We also observed the tip corner of the sample 5-a and 5-b are sharper than that of the sample 5-c. The rounded tip corners are non-retroreflective, thus corresponding to the bright dots in image 5-c. These observations can help to predict the performance of a sample.

4.2. Retroreflective property

The key concern of the reflective properties includes the retro-reflectivity and the profile of reflected beam. High and constant retroreflectivity regardless of the direction of incident light is the ideal model of retro-reflection. Practically, retro-reflection only dominates within a certain range of incident light, the reflected beam of an incident ray is slightly deviated from its incident direction, and the reflected beam is diverged into a cone of rays. For example, most of the available retro-reflective sheeting materials are not optimized for imaging optics, but for traffic control and safety applications (e.g. www.mmm.com/Scotchlite). They are relied upon to redirect the light shining from a vehicle's headlights on a traffic sign back to the driver. Therefore, the rays are reflected at an angle with respect to the incident rays, instead of onto themselves. Furthermore, to account for a range of differences between vehicles, the light rays are returned in a cone, instead of in a single direction, with virtually all the reflected rays within three degrees of the source.

These properties are commonly characterized by three angles in describing the performance of retroreflective materials in traffic control industry: entrance angle, ω_e , observation angle, ω_o , and cone angle,

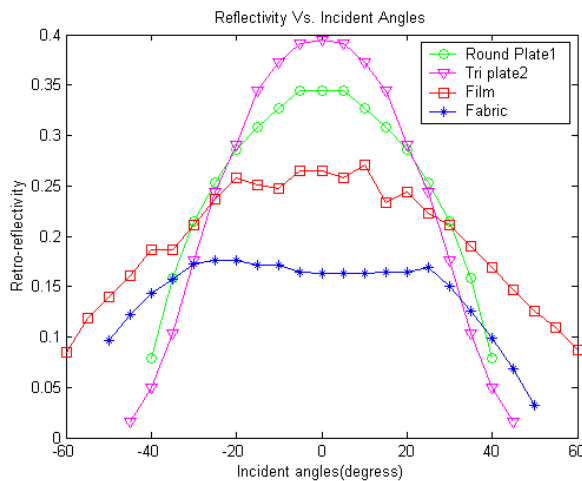
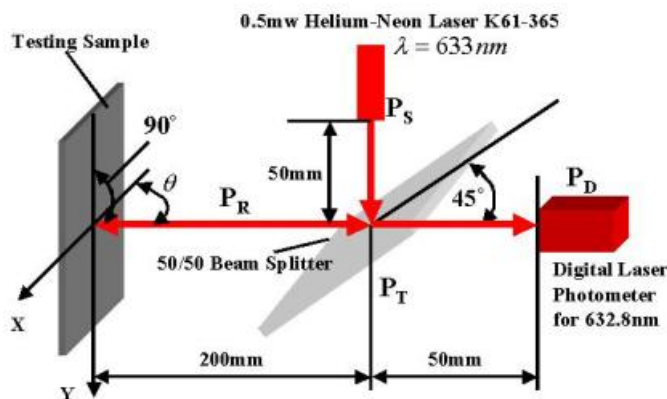


Fig.6 Evaluating the retro-reflectivity and entrance angles (a) Measurement setup illustration; (b) Relationship of retro-reflectivity with respect to incident angles

retro-reflectivity functions of the four samples relative to angles of incident rays. It demonstrates that the peak retro-reflectivity of the four samples varies from 40% to 15%, and remains constantly high within a wide range of entrance angles ($\pm 40^\circ$). The retroreflected power of the micro-bead fabric is significantly lower than those of

$\Delta\omega_o$ (Fig. 3-b). The entrance angle, defined as the angle of incidence to the surface, specifies the angular range in which a material remains highly retro-reflective. The observation angle is defined as the angular difference between the incident ray and the principal ray reflected by the surface. The cone angle, defined as the angular width of the reflected rays around the principal reflected ray, specifies the angular width of a reflected beam. A wide entrance angle, zero observation angle, and zero cone angle are preferred in HMPDs. Some of the sample materials shown in Figure 5 were designed to optimize the entrance angle and minimize the observation and cone angles to meet imaging quality, but the residuals exist.

Using the setup shown in Fig.6-a, we measured the retroreflectivity of the four samples. A 0.5mw Helium-Neon laser was used as a light source. As we tilted a retroreflective sample, a photometer was used to record the retro-reflected energy in the form of average power levels at different incident angles. The retro-reflectivity, R , is obtained by:

$$R = \frac{P_D}{P_S * t * r}$$

Where P_D and P_S are the measured retro-reflected power transmitted through the beam splitter and the light source power, respectively. t and r are the ratios of transmission and reflection of the beam splitter, respectively. Figure 6-b shows the

the other corner-cue samples, as expected, because the micro-bead sample is based on specular reflection, instead of total internal of reflection (TIR).

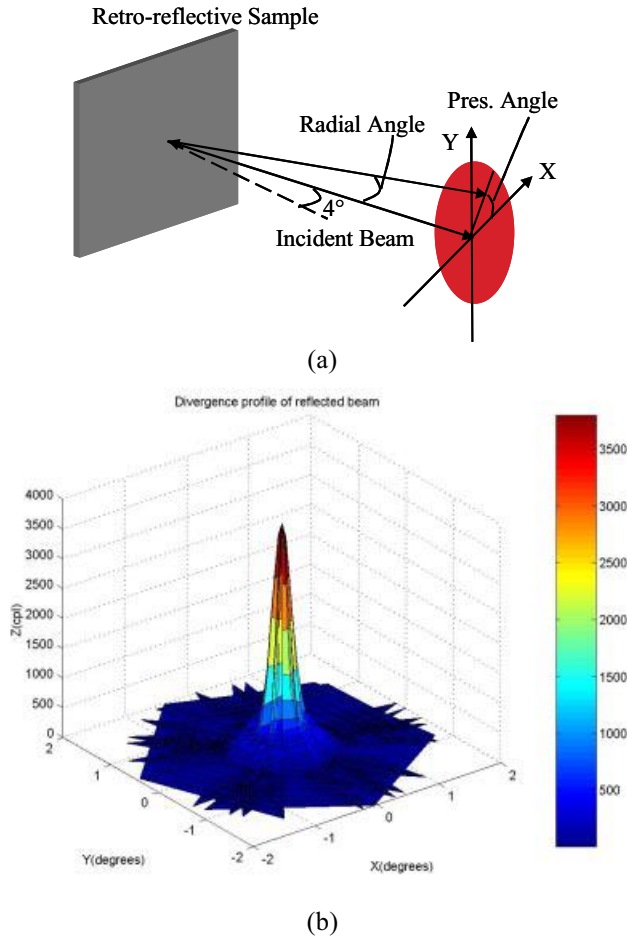


Fig.7 Evaluating divergence profile of retro-reflected beam: (a)

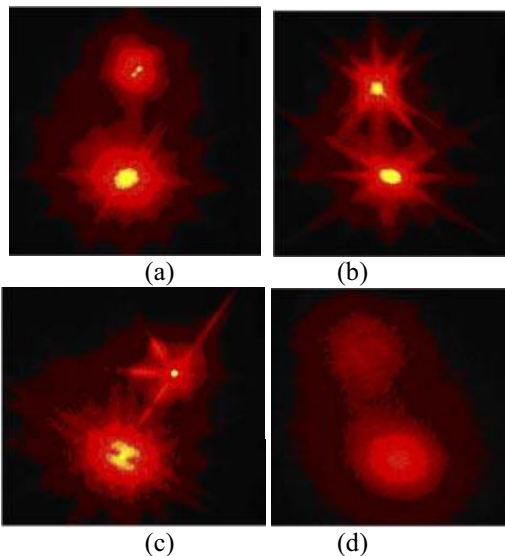


Fig. 8 Imaging properties: (a) Round sample a; (b) Triangular sample b; (c) Thin film sample c; and (d) Fabric sample d.

The reflected beam profile of the micro-corner cube film was measured by our 3M partners with their special instrument. As illustrated in Fig.7-a, the incident light is a narrow white light beam incident at 4 degrees. The energy distribution of the reflected beam is measured at sampled radial angles and presentation angles in a polar coordinate system. Radial angle is the angular distance from the central direction of the reflected beam to the measured position (i.e. the angle between the incident direction and the measured direction), and the presentation angle is the circumferential position of the measurement. 21 radial angles (from zero to 2 degrees) were measured for each presentation angle, and the presentation angle is from 0 to 360 degrees. The measurement was taken at about 250mm away from the sample. Figure 7-b shows the divergence profile of the reflected beam. The symmetric shape indicates that the observation angle is approximately zero. The energy dropped down to 25% of the peak energy at 0.2 degrees of radial position, and 1% at 0.4 degrees. Therefore, for 4-degree entrance angle, the cone angle of the reflected beam is as narrow as 0.4 degrees. We predict that

the divergence profiles will become broader as entrance angle is increased because cube apertures become more slit like at higher entrance angles and cause increased diffraction.

4.3. Other optical properties

With a similar setup as shown in Fig. 6-a, we observed the imaging properties of the four samples where the power meter was replaced by a CCD camera. Results are shown in Fig.8a-8d. We observed two essential practical challenges for optical imaging: artifact patterns due to the diffraction of the microstructures, and the formation of a ghost image due to first-surface mirror reflection. In fact, the usage of laser source exaggerates the speckle and the actual diffraction artifact in HMPDs with non-directional illumination is not so worse as the speckle with laser illumination, but diffraction artifacts are expected to

degrade image resolution in chromatic applications such as HMPDs.

On each picture, the brighter spot is the expected image, and the other spot is a ghost image caused by the first surface of the retroreflective screen, which acts as a specular reflective surface. This ghost image can be easily identified because it follows the screen's movement. Ghost images shifted away from the desired image can cause an overall decrease in image contrast and blurring of the image. To minimize ghost images, a solution is to apply antireflective coating. Another solution is to use hollow microstructures made of micromirrors, instead of microprisms. Because such structures are open, however, they are more prone to degradations due to handling and environmental factors. Fortunately, in HMPDs, due to the constraint of pupil, the ghost image is only observable for a very limited central visual field, approximately 0.5 degrees for a 12-mm pupil if the image is 1 meter away.

5. IMPACT ON HMPD IMAGING PROPERTIES

Most of the material characteristics discussed above have direct or indirect impact on imaging properties in the HMPD application. The various impacts are analyzed in this section.

Field-of-view (FOV): Wide FOV is desirable for wearable displays. The feasible FOV of an HMPD is not only constrained by that of the projective optics, but also limited by the maximum entrance angle of retro-reflective materials. In fact, to avoid significant degradation of luminance in peripheral visual fields, the maximum entrance angle of the screen used in a system sets up the upper-bound FOV of an HMPD. For example, for the four tested samples, the FOV of an HMPD should be equal or less than 80 degrees (Fig. 6-b), if a flat retroreflective screen is assumed. A concave shape of screen can help to expand the limit.

Screen shape and position: Owing to the essence of retro-reflection, a truly retro-reflective screen can be applied to any possible location in the physical space and can be tailored into arbitrary shapes without causing image blurring, introducing distortions to virtual images, or degrading image quality, while a diffusing screen does. It further indicates that no precise calibration is necessary to position a retro-reflective screen in an augmented environment. Practically, the $\pm 40^\circ$ limitation of entrance angle (Fig. 6-b) sets up the constraint of screen shape. A retro-reflective screen can be tailored into significantly curved shapes, but as approaching the marginal visual fields, the drop of reflectivity results in a gradual vignetting effects on image brightness. Therefore, for a given visual field, we predict that a concave shape can improve image brightness of marginal fields, but a convex shape will worsen the brightness of marginal fields. Analysis shows that a retro-reflective screen with non-zero observation angle leads to different image magnification if positioned at different distance from the image plane, thus such a screen can not be positioned arbitrarily without degrading image quality, and not usable in a mobile system such as HMPDs.³ The observation angle of the sample 5-c we measured is approximately zero, but the micro-bead sample has up to 3 degrees of observation angle.

Cross-talk: For an ideal retro-reflective screen, the stereo pair of images projected for the left and right eyes, or different channels of images projected for individual users, are naturally separated. Practically, the cone angle of the reflected beam is as narrow as 0.4 degrees for the measured sample (Fig. 7-b), thus crosstalk between left/right eyes can possibly occur when the user is over 9 meters away from a screen, and for such a distance no crosstalk is present if two users stand side-by-side. Therefore, it is possible to generate as many unique perspectives as needed for each user in a collaborative environment, without introducing crosstalk from any other participants. The performance of different material technologies varies and should be verified to support the above statement.

Functionally seamless augmentation: Owing to the greatly higher reflectivity of retro-reflective surfaces than diffusing surfaces, users can only perceive virtual objects when they look toward surfaces coated with the retro-reflective materials. Thus, it could be said users can naturally switch their focus of interest between the real and virtual workspaces, which will not happen in conventional optical see-through HMDs.⁶ Moreover, the combination of projection and retro-reflection makes an HMPD capable of intrinsically providing correct occlusion cues of computer-generated virtual objects by real objects. As a consequence, if a user reaches to grasp a virtual object, virtual objects behind his hand disappear naturally, as would occur in the real world.

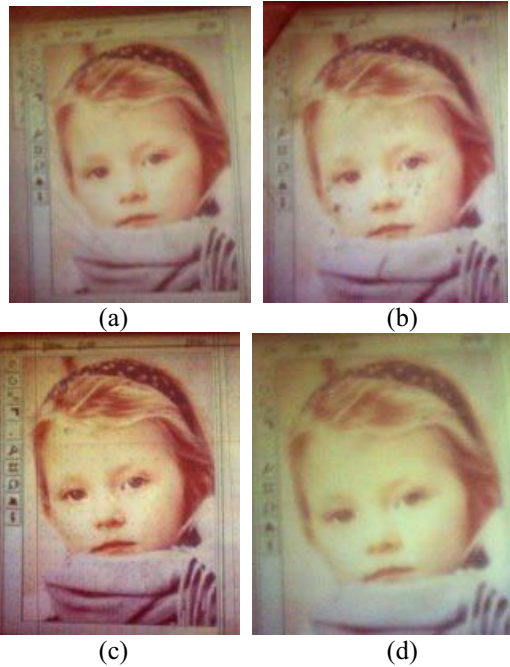


Fig. 9 Imaging performances of the four representative samples in Fig. 5a-5d

Imaging quality: Previous analysis predicted that non-zero observation angle could affect the perception of image size and depth, and the actual size and location of the exit pupil in an HMPD. It also predicted that non-zero cone angle could result in different level of image blurring with different distance away from the screen.³ The diffraction artifacts and ghost reflections would result in degradation of image resolution or blurring as well. For example, we observed that the micro-bead fabric caused much more noticeable image blurring than the micro-cube film. Figures 9-a through 9-d shows the images taken at the exit pupil of our HMPD prototype with the four different samples in Fig. 5a-5d, respectively. The image 9-c (the film with approximately zero observation angle and less than 0.4 degree divergence) formed a sharper image than the fabric 9-c.

6. CONCLUSION

The concept of head-mounted projective display (HMPD), an emerging technology lying on the boundary of conventional head-mounted displays (HMD) and projection-based displays, has been recently proposed as an alternative to optical see-through stereoscopic displays. An HMPD consists of a pair of miniature projection lenses and flat panel displays mounted on the head and retro-reflective sheeting material placed strategically in the environment. The quality and properties of the retro-reflective material play critical roles in the overall imaging quality of HMPDs. The retro-reflective sheeting material is commonly used in traffic control and photonic lighting systems, rather than optimized for imaging purpose as in the HMPDs. The size and shape of the microstructures cause artifacts on image. In this paper, we evaluated the various existing retro-reflective materials and examined how the material characteristics play their roles in an imaging system, such as the HMPD, and predicted the imaging artifacts caused by these characteristics. The maximum entrance angle of a retro-reflective screen not only sets up the upper bound FOV of HMPDs, but also set up limits to the screen shape. A concave shape is expected to improve image brightness of marginal visual fields or expand the upper bound FOV, but a convex screen would worsen the marginal visual field. The observation angle not only affects imaging quality, but screen position as well. Zero-observation is required. The cone angle determines the minimum separation of two image sources, and affects imaging quality as well. Narrow cone angle is required to ensure separation of left/right images in HMPDs. Diffraction and ghost imaging degrade image quality, but not visible in HMPDs. These findings are applicable to other imaging systems using retro-reflective arrays as well.

ACKNOWLEDGEMENTS

This paper is based on work supported by National Science Foundation Grant IIS 00-83037 ITR, the NSF IIS 00-82016 ITR, and the NSF EIA-99-86051. We would like to specially acknowledge Dr. Ken Smith from 3M Inc. for

his tremendous help on sample supply and measurement, and Miss Donna Desmarais from the Reflexite Inc. for her help on sample supply. We also would like to thank Axelle Girardot for her early work on sample assessment.

REFERENCES

- [1] Ryugo Kijima and Takeo Ojika, "Transition between virtual environment and workstation environment with projective head-mounted display", *Proceedings of IEEE 1997 Virtual Reality Annual International Symposium*, IEEE Comput. Soc. Press. 1997, pp.130-7. Los Alamitos, CA, USA.
- [2] J. Fergason. "Optical system for head mounted display using retro-reflector and method of displaying an image", U.S. patent 5,621,572. April 15, 1997.
- [3] Hong Hua, A. Girardot, Chunyu Gao, and J. P. Rolland. "Engineering of head-mounted projective displays". *Applied Optics*, 39 (22), 2000, 3814-3824.
- [4] I. Sutherland. "The ultimate display". *Proceedings of IFIP 65*, Vol. 2, 1965, pp.506-508.
- [5] C. Cruz-Neira, D. J. Sandin, T. A DeFanti. "Surround-screen projection-based virtual reality: the design and implementation of the CAVE", *Proc ACM SIGGRAPH 93 Conf Comput Graphics 1993*. Publ by ACM, New York, NY, USA, 1993. 135-142.
- [6] Rolland, J.P., and H. Fuchs, "Optical versus video see-through head-mounted displays in medical visualization," *Presence: Teleoperators and Virtual Environments (MIT Press)*, 9(3), (2000), 287-309.
- [7] Naoki Kawakami, Masahiko Inami, Dairoku Sekiguchi, Yasuyuki Yangagida, Taro Maeda, and Susumu Tachi, "Object-oriented displays: a new type of display systems—from immersive display to object-oriented displays", *IEEE SMC'99 Conference Proceedings*, 1999 IEEE International Conference on Systems, Man, and Cybernetics, Vol.5, 1999, pp.1066-9 vol.5. Piscataway, NJ, USA.
- [8] Hong Hua, Chunyu Gao, Leonard Brown, N. Ahuja, and J. Rolland, "Using a head-mounted projective display in interactive augmented environments", in *Proceedings of IEEE International Symposium on Augmented Reality 2001*, October 29-30, 2001, New York, NY.
- [9] J. P. Rolland, H. Hua, C. Gao, and F. Biocca, "Innovative Displays for Augmented Reality Applications and Remote Collaborations", *Medicine Meets Virtual Reality (MMVR)*, Newport Beach, CA January 27, 2001 (Abstract and Oral presentation).
- [10] Masahiko Inami, Naoki Kawakami, Dairoki Sekiguchi, Yasuyuki Yanagida, Taro Maeda, and Susumu Tachi, "Visuo-haptic display using head-mounted projector", *Proceedings IEEE Virtual Reality 2000*, IEEE Comput. Soc. 2000, pp.233-40. Los Alamitos, CA, USA.
- [11] J. Parsons, and J. P. Rolland, "A non-intrusive display technique for providing real-time data within a surgeons critical area of interest," *Proceedings of Medicine Meets Virtual Reality98*, 1998, 246-251.
- [12] Hong Hua, Chunyu Gao, Frank Biocca, and Jannick P. Rolland, "An Ultra-light and Compact Design and Implementation of Head-Mounted Projective Displays", *Proceedings of IEEE-VR 2001*, p. 175-182, March 12-17, 2001, Yokohama, Japan.